Magnetic properties of bimetallic AuPdO and AuPd nanoparticles confined in ordered mesoporous silica SBA-15 channels

W. Iwamoto*, G. G. Lesseux*, B. F. Dias**, A. A. Teixeira-Neto**,
E. Teixeira-Neto*** R. R. Urbano* and C. Rettori*,**

* Instituto de Física "Gleb Wataghin", UNICAMP, 13083-859
Campinas, SP, Brazil, wiwamoto@ifi.unicamp.br
** Universidade Federal do ABC, Centro de Ciências Naturais e Humanas, 09210-170
Santo André, SP, Brazil, angela.neto@ufabc.edu.br
*** Departamento de Química Fundamental, Instituto de Química - USP, 05508-000
São Paulo, SP, Brazil, erico@iq.usp.br

ABSTRACT

In this work we report on the magnetic properties of the composites bimetallic AuPdO and AuPd nanoparticles (AuPdO- and AuPd-NPs) supported on mesoporous silica SBA-15 channels (AuPdO- and AuPd-NPs/SBA-15) by means of Electron Spin Resonance and Magnetization experiments. A single magnetic resonance line was observed from 300 K down to 50 K. The normalized integrated resonance intensity remains nearly constant in the entire range of temperature.

Magnetization measurements at 300 K were able to detect magnetic loops due to the AuPdO and AuPd-NPs, in spite of the small amount of NPs ($\sim$ 1.5 % wt.) present in our samples and the relatively large intrinsic magnetization of the mesoporous silica SBA-15 supports. These results characterize the observed resonance as a ferromagnetic resonance (FMR).

Keywords: Nanoparticles, Ferromagnetism, Electron Spin Resonance, Magnetization, SBA-15, mesoporous materials

1 INTRODUCTION

Nowadays, bimetallic nanoparticles (NPs) systems became important due to the expected synergy between the two metallic species, despite the intrinsic complexity of having two interacting metallic NPs. In the bimetallic system of the alloyed Au-Pd (NPs) it was demonstrated that Pd is able to promote, for certain reactions, the catalytic activity of Au, and vice-versa [1]. In particular, materials consisting of bimetallic AuPdO and AuPd nanoparticles (AuPdO- and AuPd-NPs) supported on mesoporous silica SBA-15 channels (AuPdO- and AuPd-NPs/SBA-15) have become composite compounds of great interest due to their catalytic applications [2].

Apparently, mesoporous oxide structure with high surface area for hosting NPs of metals can dramatically improve their functionalities, such as magnetic, catalytic and optoelectronic activities [3]. From this scenario, SBA-15 is usually selected as a host material because it has well-ordered large hexagonal silica mesoporosities with high thermal stability and large surface area [4]. Morover, due to the weak interaction between silica and metal, SBA15 materials reduce the tendency to aggregate NPs.

Apart from several technological applications, another important issue is the academic study of metallic nanoparticles (NPs) supported in this silica host. The surprising discovery that gold-nanoparticles (Au-NPs) display magnetic properties, in contrast to the diamagnetic behavior of the bulk material, have stimulated many studies aimed to understand this phenomenon [5], [6]. In this work we report on the magnetic properties of these AuPdO- and AuPd NPs/SBA-15 that we believe may contribute to the understanding of both viewpoints, scientific interest and catalytic properties of these NPs composites.

2 EXPERIMENTAL DETAILS

The powder X-ray diffraction (XRD) measurements of the samples were carried out in a Phyllips Diffractometer with Cu-Kα radiation ($\lambda = 1.5418$ Å). The size and morphology of the NPs were characterized by Scanning Transmission Microscopy (SEM) measurements using a FEI Inspect F-50 field emission scanning electron microscope and the TEM micrographs were taken using a JEOL JEM-2100F transmission electron microscope at 200 kV. The magnetic characterization (M *vs* H) was performed in a SQUID magnetometer (Quantum Design MPMS) at 300 K. For the Electron Spin Resonance (ESR) measurements we used colloidal samples of NPs/SBA-15 carried out in a Bruker-ELEXSYS 500 spectrometer at X-band frequencies ($\nu = 9.48$ GHz) using a TE_{102} resonators coupled to a temperature controller of a ^{4}He-flux system for temperature down to 4.2 K.

2.1 AuPdO- and AuPd-NPs/SBA-15 samples fabrication

We have prepared the support of mesoporous silica SBA-15 according to the Zhao et al recipe [7]. At 35 °C, a solution of 4.08 g of triblock copolymer $EO_{20}PO_{70}EO_{20}$ (Pluronic 123, Aldrich) and 30 mL of deionized water was stirred until complete dissolution of the surfactant (about 30 h). Then, we added 120 mL of hydrochloric acid (2 mol L^{-1}) to the solution and kept under stirring for 1 hour. 9.1 ml of tetraethylorthosilicate (Aldrich) and maintained under stirring at 35 °C for an additional 24 h. At the end of this period the solution was placed into inox-lined teflon vessels and aged at 100 °C for a another 24 h. Then washing was performed with 2 L of deionized water and drying in an oven at 40 °C. Finally, the material was subjected to a calcination procedure at 500 °C for 12 h to remove the surfactant. Thereby, the "as-prepared" SBA-15 supports were modified with 3-aminopropyl-trimethoxysilane (APTS) following Li et. al method [8]: 1 g SBA- 15 was added to an APTS solution (3.97 x 10^{-3} mol APTS in 29.60 mL of toluene), and the mixture was heated at 80 °C in a water-condenser for 6 h. The solid was collected, washed with ethanol, and dried in air at room-T to obtain the APTS-modified SBA-15 supports (SBA-15/APTS). In order to prepare the NPs/SBA-15/APTS, 1 g of SBA-15/APTS was added to an either $HAuCl_4$ or $PdCl_2$ solution of 1 mmol/L at room-T and the mixture was heated at 80 °C in a water-condenser for 5 h. The solid product was filtered out, fully washed with distilled water (until Cl-free) and then washed with ethanol. The calcination (C) and reduction (R) procedures were similar to those adopted for preparation of 1 % Au/SBA-15 by Li et al [8]. The reactions were operated under mild conditions in air at atmospheric conditions in a continuously stirred tank reactor. Our NPs/SBA-15/APTS samples, either C or R, contain about 1.5 % of NPs determined by inductively coupled plasma atomic emission spectroscopy (ICP-AES). For simplicity we shall name SBA-15 C or R to our SBA-15/APTS C or R supports.

2.2 EXPERIMENTAL RESULTS AND DISCUSSION

Figure 1 a) presents the SEM images for the AuPdO-NPs/SBA-15 samples and Figure 1 b) displays the TEM images of AuPdO-NPs in the range of 3-6 nm within the mesoporous SBA-15 channels. Larger AuPdO-NPs are, probably, outside the mesoporous channels. Similar SEM and TEM images were obtained for the AuPd-NPs/SBA-15 samples (not shown). Figure 1 c) shows their corresponding XRD patterns. The XRD patterns show the peaks corresponding to the face-centered-cubic (FCC) of the AuPdO (black line) and AuPd (blue line) NPs.

Figures 2a) and 2b) display the field dependence of the Magnetization (M *vs* H) for the AuPdO- and AuPd-NPs/SBA-15 samples at 300 K, respectively. For comparison, the M *vs* H curves for the mesoporous silica SBA-15, C or R supports, are also shown. These data show that the AuPdO-NPs/SBA15 presents a net saturation magnetization about 3 times larger than that of AuPd-NPs/SBA15, after subtracting the SBA15 contribution.

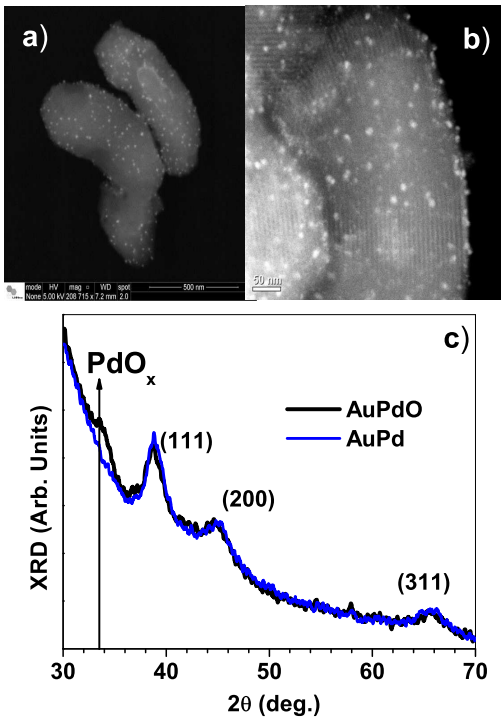

Figure 1: Representative a) and b) of SEM and TEM images, respectively, for AuPdO-NPs/SBA-15; c) XRD of the AuPdO- (black line) and AuPd-NPs/SBA-15 (blue line) samples. The indexed peaks correspond to the cubic Au structure.

We observed no evidence of superparamagnetic behavior in the zero-field cooling (ZFC) and field cooling (FC) magnetic susceptibility measurements in the range of 2 K $< T <$ 300 K (not shown). Figure 3 presents the ESR for the AuPdO- and AuPd-NPs/SB-15 samples at 300 K. For comparison, the weak ESR observed from the mesoporous silica SBA-15, C and R supports are included in these figures. The ESR spectrum of the background coming from the cavity and sample quartz tube is also displayed in this Figure 3. These ESR experiments show that a single magnetic resonance line was observed from 300 K down to 50 K. Similarly to the magnetization data of Figure 2, the resonance intensity of the AuPdO-NPs/SBA-15 sample is stronger than that of the AuPd-NPs/SB-15 one.

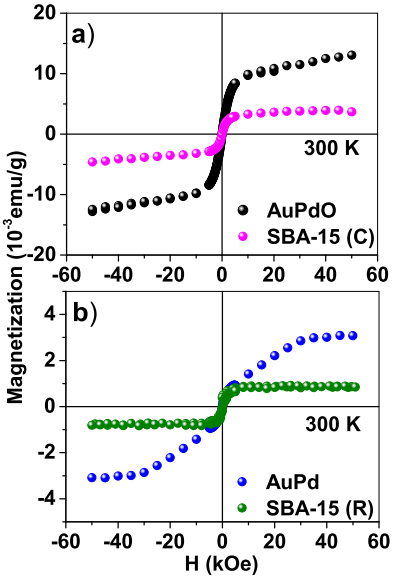

Figure 2: *M vs H* at 300 K for the AuPdO- and AuPd-NPs/SBA-15 samples. For comparison the *M vs H* curves for the mesoporous silica SBA-15 (C) and (R) supports are also shown.

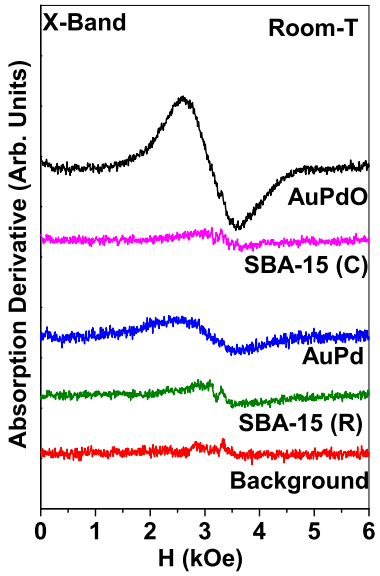

Figure 3: ESR spectra for the AuPdO- and AuPd-NPs/SBA-15 samples at 300 K. For comparison the weak ESR from the mesoporous silica SBA-15 (C) and (R) supports are also included. The ESR background coming from the cavity and sample quartz tube is displayed.

Figures 4a), 4b) and 4c) show the temperature dependence of the peak-to-peak resonance linewidth, ΔH_{PP}, field for resonance, H_r, and normalized integrated resonance intensity, $I/I(300\ \mathrm{K})$, respectively, for the resonances of Figure 3. These data show that at low-T $\Delta H_{PP}(T)$ increases, $H_r(T)$ decrease, however $I(T)/I(300$ K) remains nearly constant in the entire T-range. These results clearly characterize the observed resonance as FMR, in contrast to the scenario of active ESR paramagnetic defect centers suggested by E. Rombi, et. al. [9] in their Au/SBA-15 samples.

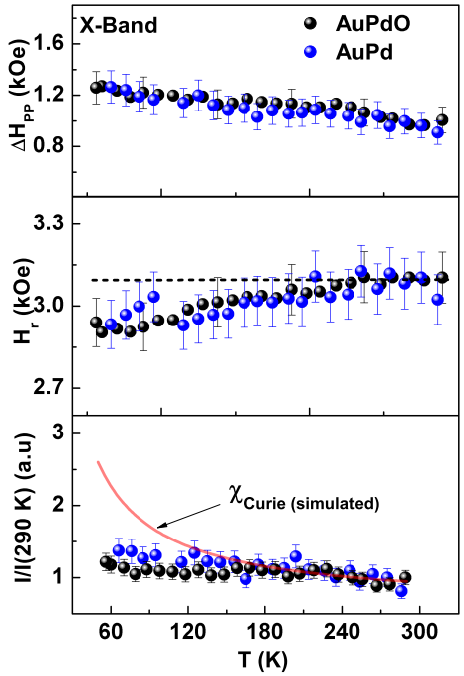

Figure 4: For the AuPdO- and AuPd-NPs/SBA-15 samples, temperature dependence of: a) the peak to peak resonance line width, $\Delta H_{PP}(T)$; b) field for resonance, $H_r(T)$; and c) normalized integrated resonance intensity, $I(T)/I(300$ K). The Curie-law (red line) is plotted in c) for comparison.

Note that a very weak and broad X-Band ESR signal is observed near $g \sim 2$ (3.2 kOe) in the SBA-15 (C) and SBA-15 (R) supports. Since no Fe element was found by Energy-dispersive X-ray spectroscopy (EDS) analysis (not shown), this weak ESR signal may be associated to others ESR active impurities, as the super-oxide $\equiv$ Si–O–O, for example [10]–[13]. Despite these possibilities, all our ESR and Magnetization results and analysis lead us to conclude that our AuPdO- and AuPd-NPs/SBA-15 samples present a ferromagnetic behavior.

3 CONCLUSIONS

In summary, we have shown that our AuPdO- and AuPd-NPs/SBA-15 samples present a ferromagnetic behavior which was found and confirmed by means of magnetization and ESR experiments as a function of temperature. We argue that the origin for the magnetism in these bimetallic NPs may be associated to a weak type of covalent bonds between the metallic NPs and the Si and/or O atoms of the mesoporous silica SBA-15 supports. The magnetic nanoparticles (AuPdO and AuPd-NPs) confined in ordered mesoporous silica SBA-15 channels can lead to a magnetic-coupling interaction, which could enhance the magnetic properties of these bimetallic AuPdO- and AuPd-NPs/SBA-15 nanocomposites [14]. Then, we suggest that the catalytic efficiency of these AuPdO- and AuPd-NPs may be mainly associated to the affinity and/or facility that these metallic NPs have in promoting covalent bonds and that the catalytic activity may possible be quantified by the intensity of the FMR.

ACKNOWLEDGEMENTS

The TEM data was acquired in the LME/LNNano at the Brazilian Synchrotron Light Laboratory (LNLS) and CEM-UFABC. The authors thank FAPESP (SP-Brazil), CNPq and CAPES (Brazil), for supporting this work.

REFERENCES

[1] Dimitratos, N.; Lopez-Sanchez, J.A.; Hutchings, G. J.: Chem. Sci. 3, 20, (2012).

[2] Raveendran Shiju, N.; Guliants, Vadim V.: Appl. Catal. A; General 356, 117 (2009).

[3] B.M. Yang, M. Kalwei, F. Schuth, K.J. Chao, Appl. Catal. A Gen.254, 289 (2003).

[4] Zhao, D.; Feng, J.; Huo, Q.; Melosh, N.; Fredrickson, G. H.; Chmelka B. F., Stucky G. D.: Science 279, 548 (1998).

[5] Lesseux, G. G.; Iwamoto, W.; Rosas,V.; Vautier-Giongo, C.; Rettori, D.; Urbano, R. R.; Rettori, C: Ferromagnetic resonance in amine/organic acid capped Au-nanoparticles assisted by yttrium-oxide. In: NSTI-Nanotech, Santa-Clara, proceedings, 2012.

[6] Roldn, A.; Illas, F.; Tarakeshwar, P.; Mujica, V.: J. Phys. Chem. Lett., 12, 2996, 2011.

[7] D. Zhao, Q. Huo, J. Feng, B. F. Chmelka, G. D. Stucky: J. Am. Chem. Soc. (1998), 120, 6024.

[8] Li, L.; Jin, C.; Wang, X.; Ji, W.; Pan, W.; Knaap, T.; Stoel, R.: Catal. Lett. (2009), 129, 303.

[9] Rombi, E.; Cutrufello, M. G.; C. Cannas, M.; Occhiuzzi, B.; Ferino, I.: Phys. Chem. Chem. Phys., 14, 68896897, (2012).

[10] Weeks, R.A.; J. Appl. Phys. 27, 1376, (1956).

[11] Trejda, M.; Ziolek, M.; Decyk, P.; Duczmal, D.: Microporous and Mesoporous Materials 120, 214220, (2009).

[12] Griscom, D.L.; Friebele, E.J.: Phys. Rev. B 24, 4896, (1981).

[13] Friebele, E.J.; Griscom, D.L.; Stapelbroek, M.; Weeks, R.A. Phys. Rev. Lett., 43, 1346, (1979).

[14] Wang, P. F.; Jin, H. X.; Chen, M.; Jin, D. F.; Hong, B.; Ge, H. L.; Gong, J.; Peng, X. L.; Yang, H.; Liu, Z. Y.; Wang, X. Q.: Journal of Nanomaterials, Volume 2012, Article ID 269861, 7 pages, (2012).